Received: 25 November 2016 | Revised: 8 February 2017 | Accepted: 12 February 2017

DOI 10.1002/jobm.201600692

Journal of Basic Microbiology

RESEARCH PAPER

Structural analysis and enhanced production of fusaricidin from *Paenibacillus kribbensis* CU01 isolated from yellow loess

Jaewon Ryu[1] | **Jong M. Kim**[1] | **Chul W. Lee**[2] | **Si W. Kim**[1,3]

[1] Department of Energy Convergence, Chosun University, Gwangju, Republic of Korea

[2] Department of Chemistry, Chonnam National University, Gwangju, Republic of Korea

[3] Department of Environmental Engineering, Chosun University, Gwangju, Republic of Korea

Correspondence
Si Wouk Kim, Department of Environmental Engineering, Chosun University, 309 Pilmundaero, Gwangju 61452, Republic of Korea.
Email: swkim@chosun.ac.kr

Funding information
Ministry for Food, Agriculture, Forestry, and Fisheries, Grant number: 112003-3; Bio-industry Technology Development Program 2012; Research Fund of the Chosun University 2014

A bacterial strain showing strong antifungal activity was isolated from yellow loess and was identified as *Paenibacillus kribbensis* CU01. Insoluble mucoidal polymers were separated from M9 culture medium via low-speed centrifugation. Most antifungal activity was associated with substances in the insoluble precipitate, which was purified by reverse phase high performance liquid chromatography. Purified fractions were analyzed using matrix-assisted laser desorption/ionization time-of-flight/time-of-flight mass spectrometry. Two major ion peaks with mass-to-charge ratio values (*m/z*) at 883.6 and 897.6 were revealed. After alkaline hydrolysis and sequence analysis, two cyclic depsipeptides were identified as, fusaricidin A and fusaricidin B. Their production was significantly increased by the addition of glucose, Fe^{2+}, and Mn^{2+} to M9 medium. Maximum concentrations of produced fusaricidin A and fusaricidin B at flask-scale comprised 460 mg L^{-1} and 118 mg L^{-1}, respectively: the highest production concentrations yet reported in the literature. This demonstrates that *P. kribbensis* CU01 has enormous commercial potential for the mass production of fusaricidin.

KEYWORDS
antifungal substance, fusaricidin, glucose, metal ions, *Paenibacillus kribbensis*, structural analysis

1 | INTRODUCTION

In agriculture, plant pathogenic fungi are responsible for significant crop losses and reduction in the quality and safety of products. Up to now, farmers have mainly relied on synthetic pesticides to control phytopathogenic fungi, but intensive use of synthetic agrochemicals has resulted in the deterioration of soil structure [1] and increase in the number of agrochemical-resistant phytopathogens [2]. For these reasons, biological control of phytopathogens by microorganisms has gained attention as a reliable alternative to the use of hazardous agrochemicals [3].

The most important point in the development of bio-control techniques against phytopathogenic fungi is the isolation of bacteria that have strong antifungal activity. In natural soil, microorganisms have evolved as long-standing communities that produce various substances for mutual competition or cooperation. Because microbial production of these substances is affected by environmental factors, target microorganisms should be isolated from samples of the soil with unique conditions. Yellow loess contains higher concentrations of silica and iron oxide, and but less organic material, than normal soil [4]. Zeng et al. demonstrated that the dominant taxonomic classes observed in loess soils were *Actinobacteria*, *Alphaproteobacteria*, *Chloroflexia*, *Acidobacteria*, and *Betaproteobacteria*. In addition, they also demonstrated that *Actinobacteria* and *Proteobacteria* were

Abbreviations: CID, collision-induced dissociation; GHPD, 15-guanidino-3-hydroxypentadecanoic acid; MALDI, matrix-assisted laser desorption/ionization; MS/MS, tandem mass spectrometry; PDA, potato dextrose agar; RP-HPLC, reversed phase high performance liquid chromatography; TFA, trifluoroacetic acid; TOF, time-of-flight; TSA, tryptic soy agar; TSB, tryptic soy broth.

two most abundant groups, and their relative abundance highly correlated with soil moisture, carbon/phosphorus ratio, pH, total phosphorus and mean annual precipitation [5].

Generally, among a wide variety of soil microorganisms, *Bacillus* and *Paenibacillus* species are known to produce various active antifungal substances that have the potential to replace chemical fungicides [6]. Although these organisms are capable of synthesizing many organic compounds, including polyenes and terpenoids, their main biosynthetic products are lipopeptides: linear or cyclic peptides containing a lipophilic hydrocarbon tail on the N-terminus. Bacterial lipopeptides are secondary metabolites, generally synthesized by non-ribosomal peptide synthetase. Fusaricidin-type antifungal compounds consist of a group of cyclic depsipeptides with molecular weights of 883, 897, 948, and 961 Da, with an unusual 15-guanidino-3-hydroxypentadecanoic acid moiety attached to a free amino group [7]. Fusaricidin shows strong antimicrobial activity against Gram-positive bacteria and fungi, but exhibits weak antimicrobial activity against Gram-negative bacteria [6]. It also shows relatively low toxicity toward ddY mice [8]. Fusaricidin inhibits growth of pathogenic bacteria at low minimum inhibitory concentrations, whereas hemolytic activity of fusaricidin was observed only at high concentrations of the substance [9]. These properties make fusaricidin an excellent candidate for medical use. Furthermore, it has been recently reported that this compound very effectively inhibits fungi that cause diseases of crops such as canola and red pepper [8,10].

Metal ions are known to play a vital role in controlling growth and production of secondary metabolites in microorganisms [11]. For example, Mn^{2+}, Mg^{2+}, Fe^{2+}, and Co^{2+} increase bacitracin production in *Bacillus licheniformis* by enhancing the activity of bacitracin synthethase [12]. Fe^{2+}, Cu^{2+}, and Zn^{2+} promote growth and antibiotic production in *Streptomyces galbus* [13], whereas Ni^{2+} inhibits growth, pigment production, and antibiotic production in this bacterium [14]. *Streptomyces* species require Fe^{3+} to produce actinomycin, neomycin, streptomycin, and chloramphenicol [15]. Similarly, Mn^{2+} has a significant effect on growth and bulbiformin production by *Bacillus subtilis* [16]. Furthermore, Co^{2+} was shown to increase prodigiosin biosynthesis by *Streptomyces coelicolor* [17]. Several metal cations significantly promote the production of fusaricidin by *Bacillus polymyxa*, with a maximum yield concentration of 20.6 mg L^{-1} [18,19].

In this study, we isolated several bacterial strains from yellow loess that inhibited growth of various phytopathogenic fungi. Morphological, biochemical, and 16S rRNA gene analyses were carried out to identify the finally isolated bacterium. For commercial purposes, a simple separation process to isolate antifungal substances from culture broth was also investigated. Structural analysis of the purified substances was then performed using MALDI-TOF mass spectrometry. In addition, the effects of adding metal ions and/or glucose to culture media for mass production of antifungal substances were also determined.

2 | MATERIALS AND METHODS

2.1 | Screening, culture media, and microorganisms

A total of 165 loess soil samples were collected from 32 different sites in Jeollanam-do province, South Korea. One gram of each soil sample was suspended in a 250 ml flask containing tryptic soy broth (TSB) and then incubated while shaking for 7 days at 30 °C. An aliquot of the turbid suspension was then transferred to fresh medium and incubated as before. After three times transfers, 100 µl of the suspension was spread onto a tryptic soy agar (TSA) plate. Colonies with different morphological appearances were chosen from countable plates and streaked on to fresh TSA plates to obtain pure cultures. *Fusarium oxysporum* KACC 40031, a fungus which causes plant wilt disease, was cultured on PDA plates for 5 days at 28 °C. Antifungal activity was assayed on PDA plates by placing a 5 mm mycelial plug in the middle of the plate and then inoculating isolated bacterial strains onto paper disks placed between the edge of the plate and mycelial plug. After pre-screened bacterial colonies were tested for antifungal activity against *F. oxysporum* KACC 40031, 14 colonies were isolated. These bacterial strains were again tested for their potential to inhibit growth of several other plant pathogenic fungi, such as *Sclerotinia sclerotiorum* KACC404579 (a causal agent of rot disease), *Phytophthora capsici* KACC40157 (a causal agent of blight disease), and *Botrytis cinerea* KACC40574 (a causal agent of gray mold disease). The pathogenic fungi used in this study were provided by the Korean Agricultural Culture Collection (KACC), Suwon, South Korea. Inhibition of fungal growth was determined by the relative sized of clear zones on the plate. Finally, the bacterial strain that showed the largest clear zones in tests with four fungi was isolated and stored in 25% (v/v) glycerol at − 80 °C for further study.

2.2 | Morphological, biochemical and molecular identification of the isolate

Morphological characteristics of the isolated bacterial strain were examined with a field emission scanning electron microscope (JSM-7500F, Oxford, UK) at an accelerating voltage of 3 kV. Taxonomic characterizations of the bacterial strain was performed on the basis of biochemical tests for oxidase, gelatin hydrolysis, starch hydrolysis, nitrate reduction, urea hydrolysis, casein hydrolysis, and ability to utilize carbon sources such as $_{L}$-arabinose, $_{D}$-cellobiose, $_{D}$-glucose, lactose, $_{D}$-mannose, melibiose, $_{D}$-raffinose, $_{D}$-sorbitol,

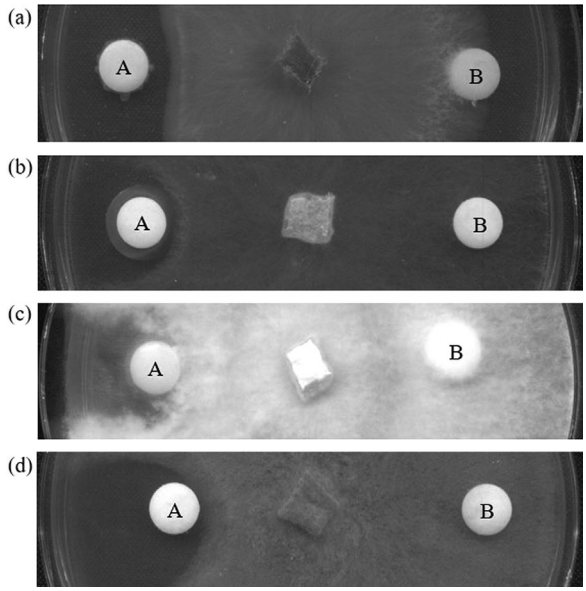

FIGURE 1 Antifungal activity of the strain CU01 against several plant pathogenic fungi (a: *F. oxysporum*; b: *S. sclerotiorum*; c: *P. capsici*; and d: *B. cinerea*). Aliquots of culture broth of strain CU01 (A) or uncultured TSB medium (B) were immersed on a paper disc

$_L$-rhamnose, $_D$-xylose, $_D$-trehalose, $_D$-mannitol, adonitol, maltose, and sucrose . The results of these tests were scored as either positive or negative.

Molecular identification was based on 16S rRNA gene sequence of the isolate determined by PCR analysis of the colony. Each PCR reaction mixture contained a small quantity of isolated cells pre-grown overnight in TSA medium, 1 μl of each of the universal primers (50 pmol μl^{-1}) 27F (5′-AGAGTTT-GATCMTGGCTCAG-3′) and 1492R (5′-TACGGY-TACCTTGTTACGACTT-3′), 4 μl of dNTP mix (2.5 mM each), 5 μl of 10 × PCR buffer (TaKaRa, Japan), 38.75 μl of dd H_2O, and 0.25 μl of TaKaRa Ex Taq DNA polymerase (5 U μl^{-1}). PCR conditions were as follows: one cycle for 5 min at 98 °C; then 30 cycles for 30 s at 95 °C, 30 s at 55 °C, and 90 s at 72 °C; and finally 10 min at 72 °C. Amplified 16S rRNA gene was purified using a commercial DNA purification kit (QIAGEN, Germany), ligated to the pCR2.1 vector (Invitrogen, USA), and transformed into *E. coli* DH5α cells via chemical transformation. The recombinant plasmid was prepared from 10 ml of overnight culture in LB medium using silica spin columns (PureLink Quick Plasmid Miniprep kit; Invitrogen, USA) and sent for sequencing (Macrogen, Korea).

2.3 | Cultivation and production of antifungal substances

A colony of each bacterial strain was inoculated in a 250 ml flask containing 50 ml of TSB medium, and incubated at 30 °C with an agitation speed of 180 rpm for 24 h to create a seed culture. With the economic considerations of mass production in mind, M9 medium (Na_2HPO_4 6 g L^{-1}; KH_2PO_4, 3 g L^{-1}; NaCl, 0.5 g L^{-1}; NH_4Cl 1 g L^{-1}; $MgSO_4$, 1 mM; $CaCl_2$, 0.1 mM; glucose, 2 g L^{-1}) was used as a cheap medium. One liter of M9 medium supplemented with 1×10^{-5} mol L^{-1} of $MnCl_2$ was inoculated with seed culture broth to a concentration of 1% (v/v) and incubated at 30 °C in a shaking incubator at 180 rpm for 3 days.

TABLE 1 Comparison of morphological and biochemical characteristics

Characteristics	Strain CU01	*P. kribbensis* AM49 T[a]
Cell shape	Rod	Rod
Cell size (μm)	0.7–0.8 × 3.9–5.1	1.5–1.8 × 4.0–7.0
Oxygen requirement	Facultative anaerobic	Facultative anaerobic
Endospore staining	+	+
Gram stain	+/–	+/–
Nitrate reduction	+	+
Gelatin hydrolysis	+	+
Starch hydrolysis	+	+
Urea hydrolysis	-	-
Casein hydrolysis	+	+
Oxidase	-	-
Sole carbon and energy source		
$_L$-arabinose	+	+
$_D$-xylose	+	+
$_D$-glucose	+	+
$_D$-mannose	+	+
$_L$-rhamnose	+	+
$_D$-cellobiose	+	+
Lactose	+	+
Maltose	+	+
Melibiose	+	+
$_D$-raffinose	+	+
Sucrose	+	+
$_D$-trehalose	+	+
$_D$-mannitol	+	+
$_D$-sorbitol	-	-
Adonitol	-	-

[a]Data for *P. kribbensis* AM49 obtained from Yoon et al. [32]

2.4 | Extraction and purification of antifungal substances

Although the culture broth was centrifuged at a relatively low speed at 3,000*g* for 10 min, most of the insoluble mucoidal polymer, which was suspended in the culture broth, was collected. Each sample of the supernatant and insoluble mucoidal precipitate was extracted with an equal volume of *n*-butanol at room temperature for 3 h. Each extract was concentrated using a rotary evaporator (R-205 rotary evaporator; Buchi, Switzerland), and the residue was dissolved in 10 ml of methanol. Because more than 95% of the antifungal activity present was ultimately mediated by the extract of mucoidal precipitate, all subsequent purification

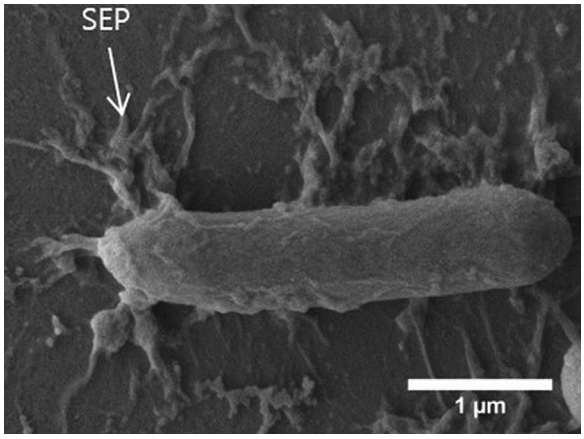

FIGURE 2 Field emission scanning electron microscope images of *Paenibacillus kribbensis* CU01 and secreted extracellular polymers (SEP). Bar size indicated 1 μm

work described in this study was performed solely using the precipitate. Crude extract was fractionized by reversed phase high performance liquid chromatography (RP-HPLC; Agilent 1200series, USA) using a ZORBAX SB-C18 column (150 mm × 4.6 mm; Agilent, USA) [7,20]. Elution was monitored using a diode array detector (Agilent, USA) at 215 nm, and major fractions were collected. The fractions exhibiting antifungal activity were vacuum evaporated to dryness. To determine whether antifungal lipopeptides contained a lactone linkage, the fractions were dissolved in 1 M KOH and allowed to react for 1 h at room temperature [21]. The reactants were purified by RP-HPLC by a previously described method. The products were characterized by MALDI-TOF mass spectrometry analysis.

2.5 | MALDI-TOF mass spectrometry analysis

Mass spectrometry analysis was performed using an UltrafleXtreme MALDI mass spectrometer (Bruker, USA) with smartbeam2 using a 1,000 Hz modified Nd-YAG laser (excitation wavelength: 337 nm) for desorption and ionization. Each sample of purified antifungal substance treated with/without KOH was mixed with an equal volume of matrix solution (a saturated solution of α-cyano-4-hydroxycinnamic acid in 50% aqueous acetonitrile containing 0.1% TFA), spotted on the target, air dried, and measured. Spectra were obtained by positive ion detection in reflector mode. Monoisotopic masses were detected. Sequence analyses of the antifungal substances were performed by MALDI-LIFT-TOF/TOF mass spectrometry in CID mode. The following instrument parameters were used:

1. For recording of mass spectra in the range of 500-5,000 Da: acceleration voltage: ion source 1: 25 kV; ion source 2: 22.6 kV. Reflector voltage: reflector 1: 26.45 kV, reflector 2: 13.35 kV.
2. For the generation of MS/MS fragment spectra: acceleration voltages: ion source 1:7.72 kV; ion source 2: 7.04 kV. Reflector voltages: reflector 1: 29.5 kV; reflector 2: 13.95 kV. LIFT 1: 17 kV; LIFT 2: 4.1 kV.

2.6 | Effect of metal ions and glucose on the production of antifungal substances

The effect of metal ions on the production of antifungal substances were determined using M9 medium with the addition of 1×10^{-7}–1×10^{-2} mol L^{-1} metal ions ($FeSO_4$, $MnCl_2$, $NiCl_2$, $CoCl_2$, and $ZnSO_4$). A volume of 1 ml seed

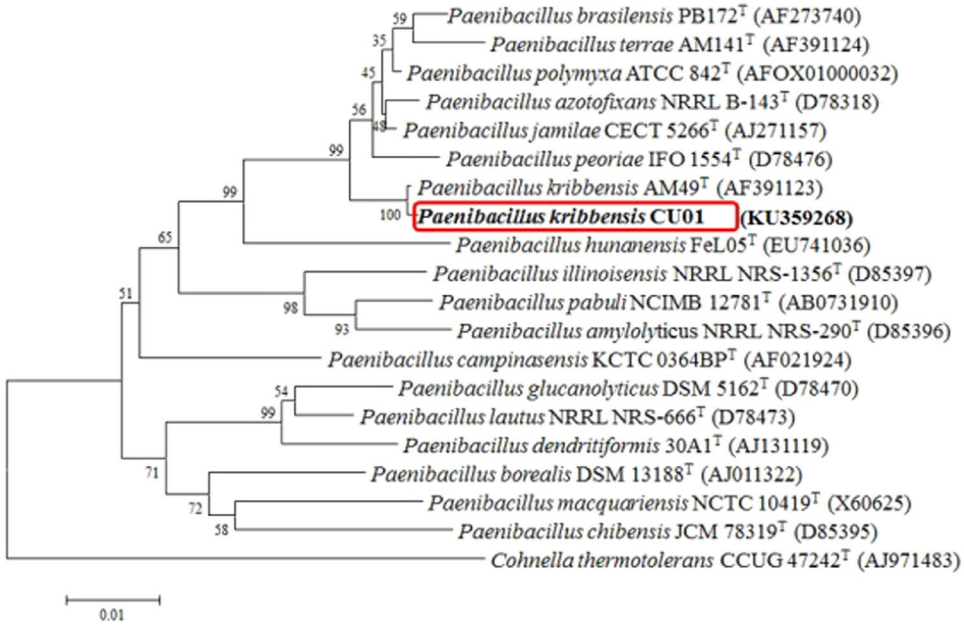

FIGURE 3 Phylogenetic tree reconstructed using the neighbor-joining method based on 16S rRNA gene sequences, showing the relationship between strain CU01 and related species of genera *Paenibacillus*. Bootstrap values (>50% from 1,000 replicates) are indicated at branching points. *Cohnella thermotolerans* CCUG47242T was used as an outgroup. Scale bar, 0.01 nucleotide substitutions per nucleotide position

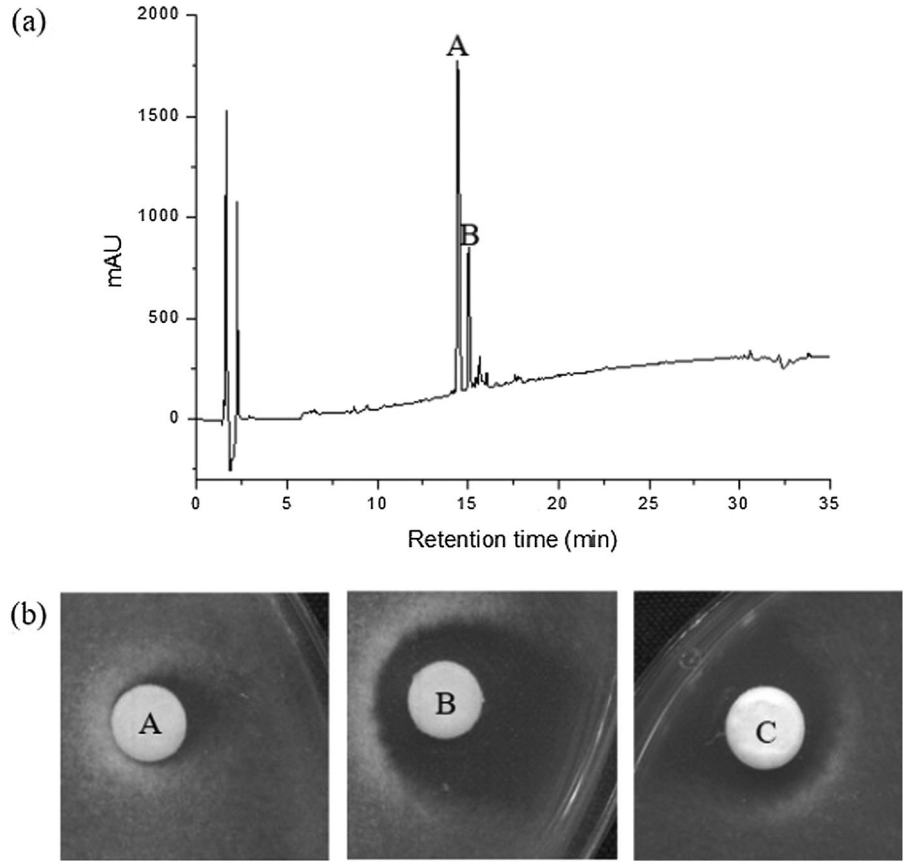

FIGURE 4 Purification of the extract of mucoidal precipitate by RP-HPLC (a) and antifungal activities of eluted fractions against *S. sclerotiorum* (b). Fractions were eluted at 14.3 min (A) and 15.0 min (B). Mucoidal precipitate extract (C) was used as a control

culture broth, which was grown in TSB medium, was used to inoculate a 250 ml flask containing 50 ml modified M9 medium into which different concentrations of metal ions had already been added. After incubation at 30 °C for 24 h, antifungal substances were extracted and thereafter, their active concentrations were quantitatively determined by RP-HPLC. At the same time, the effect of glucose on the production of antifungal substances was studied. Glucose at concentration of 2-24 g L^{-1} was added to the modified M9 medium that contained 1×10^{-5} mol L^{-1} $MnCl_2$. Cell cultivation and extraction of antifungal substances were carried out by the methods described above. The fusaricidins were quantified and compared with standards using RP-HPLC. The standards were developed using 50-1,000 μg ml^{-1} of previously purified fusaricidins in methanol [19].

3 | RESULTS

3.1 | Isolation and characterization of an antifungal bacterium

After several iterations of enrichment cultures of bacteria isolated from yellow loess, 14 bacterial strains with high antifungal activity against the plant pathogenic fungus *F. oxysporum* KACC40031 were selected for further experiments. These isolates were then tested against other potent plant pathogenic fungi, such as *S. sclerotiorum* KACC40457, *P. capsici* KACC40157, and *B. cinerea* KACC40574. As a result of these screening procedures, one strain, which was characterized by quick growth and strong antifungal activity toward a diverse array of plant pathogenic fungi, was retained (Fig. 1) and designated "strain CU01."

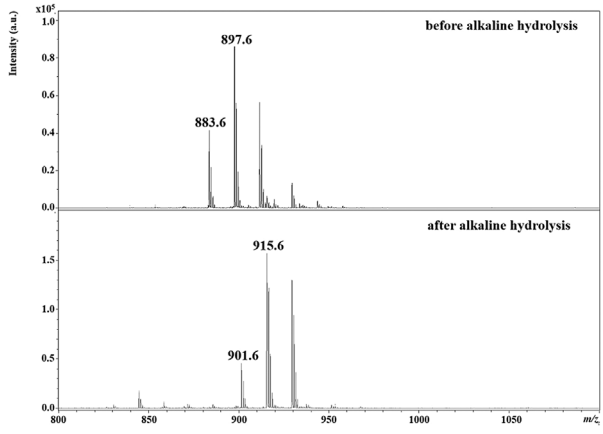

FIGURE 5 Mass shift of purified antifungal substances before and after alkaline hydrolysis

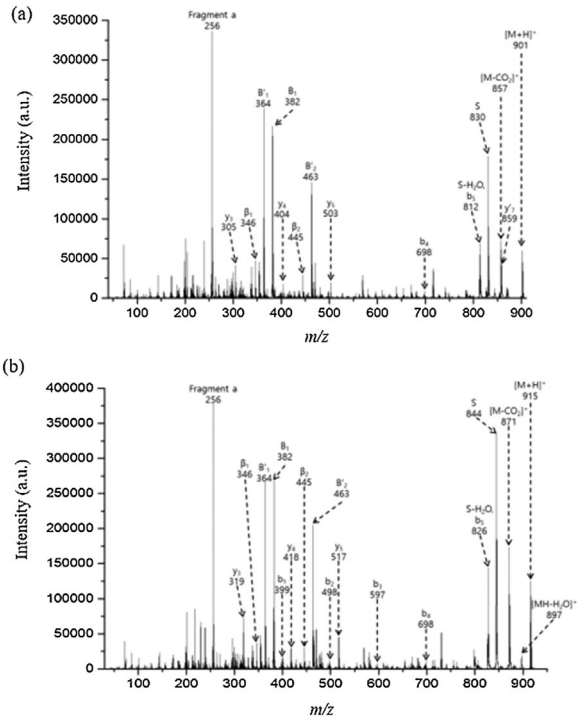

FIGURE 6 MALDI-TOF MS/MS spectra of linearized fusaricidin at m/z 901.6 (a) and 915.6 (b)

Morphologically, strain CU01 was a Gram-variable, endospore-forming, facultatively anaerobic, and rod-shaped (0.7-0.8 × 3.9-5.1 μm) bacterium (Table 1, Fig. 2). Biochemical characteristics of strain CU01 are outlined in Table 1. In particular, strain CU01 was able to reduce nitrate to nitrite and to hydrolyze gelatin, starch, and casein. Oxidase activity was absent. Strain CU01 utilized $_D$-glucose, lactose, sucrose, $_L$-arabinose, $_D$-raffinose, maltose, and $_D$-cellobiose, but could not utilize $_D$-sorbitol or adonitol (Table 1). The sequence of 16S rRNA gene of strain CU01 (NCBI accession no. KU359268) showed 99.52% similarity to that of *P. kribbensis* AM49^T (AF391123). Based on the morphological, biochemical, and phylogenetic analyses, the isolate was classified as *Paenibacillus kribbensis* CU01 (Fig. 3).

3.2 | Extraction and purification of antifungal substances

During shaking incubation of *P. kribbensis* CU01, it was found that growing cells dispersed evenly in the medium up until they reached late exponential phase. However thereafter, they secreted extracellular polymers (Fig. 2), became aggregated, and formed a large mucoidal mass. This insoluble mucoidal mass could be easily separated from the culture broth, with a low speed centrifugation at 3,000*g* for 10 min at 4 °C. After extractions of the supernatant and mucoidal precipitate were performed with *n*-butanol, strong antifungal activity of the insoluble mucoidal precipitate extract was detected. Concomitantly, RP-HPLC chromatograms showed that the fractions eluted at 14.3 and 15 min had antifungal activity. These fractions were obtained from the extract of mucoidal precipitate, and they were absent in the supernatant extract (Fig. 4).

3.3 | Structural analysis

The chemical structures of purified antifungal substances were analyzed by MALDI TOF/TOF mass spectrometry. Although there were several mass peaks in the spectrum of purified fractions, the major peaks for our primary substances of interest appeared with *m/z* at 883.6 and 897.6, respectively (Fig. 5). To clarify the structure, MS/MS analysis was carried out; however, it was not effective for sequencing our antifungal substances, because of the lack of fragmentation information. This implied that the substances were cyclic compounds.

Alkaline hydrolysis is a well-known method for breaking lactone linkage within cyclic peptides [22]. Therefore, we carried out alkaline hydrolysis of the purified antifungal substances to determine whether they were cyclic peptides. After mass spectrometry analysis, two peaks with *m/z* at 901.6 and 915.6 were observed (Fig. 5), and these values of *m/z* were consistent with the expected values of linearized fusaricidin A and B [23]. The difference in mass between the substances that had undergone alkaline hydrolysis and the intact antifungal substances was 18 Da, suggesting that the compounds have ring structures that can be opened by alkaline hydrolysis.

The MS/MS spectra of each protonated precursor ion (*m/z* 901.6, 915.6) showed various b_n, y_n,-series ions, and they also showed B_n, B_n, $ß_n$ −series ions (Fig. 6a and b). The mass peak exhibiting the highest intensity in the LIFT-TOF/TOF spectra amongst all of our investigated linearized compounds was always found at *m/z* 256.2. This peak can be attributed to the fragment ion formed by CID mode cleavage of the GHPD chain, between the α- and β-position [24]. The MS/MS spectra of precursor ion $[M + H]^+ = 901.6$ showed fragment ions *m/z* at 698 (b_4), 812 (b_5), 305 (y_3), 404 (y_4), 503 (y_5), 382 (B_1), 364 (B_1), 463 (B_2), and 830 (S) (Fig. 6a). The masses of fragment ions at *m/z* 399 (b_1), 498 (b_2), 597 (b_3), 698 (b_4), 826 (b_5), 319 (y_3), 418 (y_4), 517 (y_5), 382 (B_1), 364 (B_1), 463 (B_2), 844 (S) in the MS/MS spectrum of the precursor ion $[M + H]^+ = 915.6$ were also determined (Fig. 6b).

3.4 | Effects of metal ions on the production of fusaricidin

In the presence of 1 mM $FeSO_4$ in M9 medium, *P. kribbensis* CU01 produced fusaricidin A and fusaricidin B at concentrations of 195 mg L^{-1} and 146 mg L^{-1} (Fig. 7a). In the presence of 1 μM $MnCl_2$, *P. kribbensis* CU01 synthesized fusaricidin A and fusaricidin B at concentrations 127 mg L^{-1} and 117 mg L^{-1}, respectively. However, no fusaricidin was detected in M9 medium in the absence of metal ions. Notably, salts such as $NiCl_2$, $CoCl_2$, or $ZnSO_4$, did not stimulate fusaricidin production as much as did $FeSO_4$. As shown in

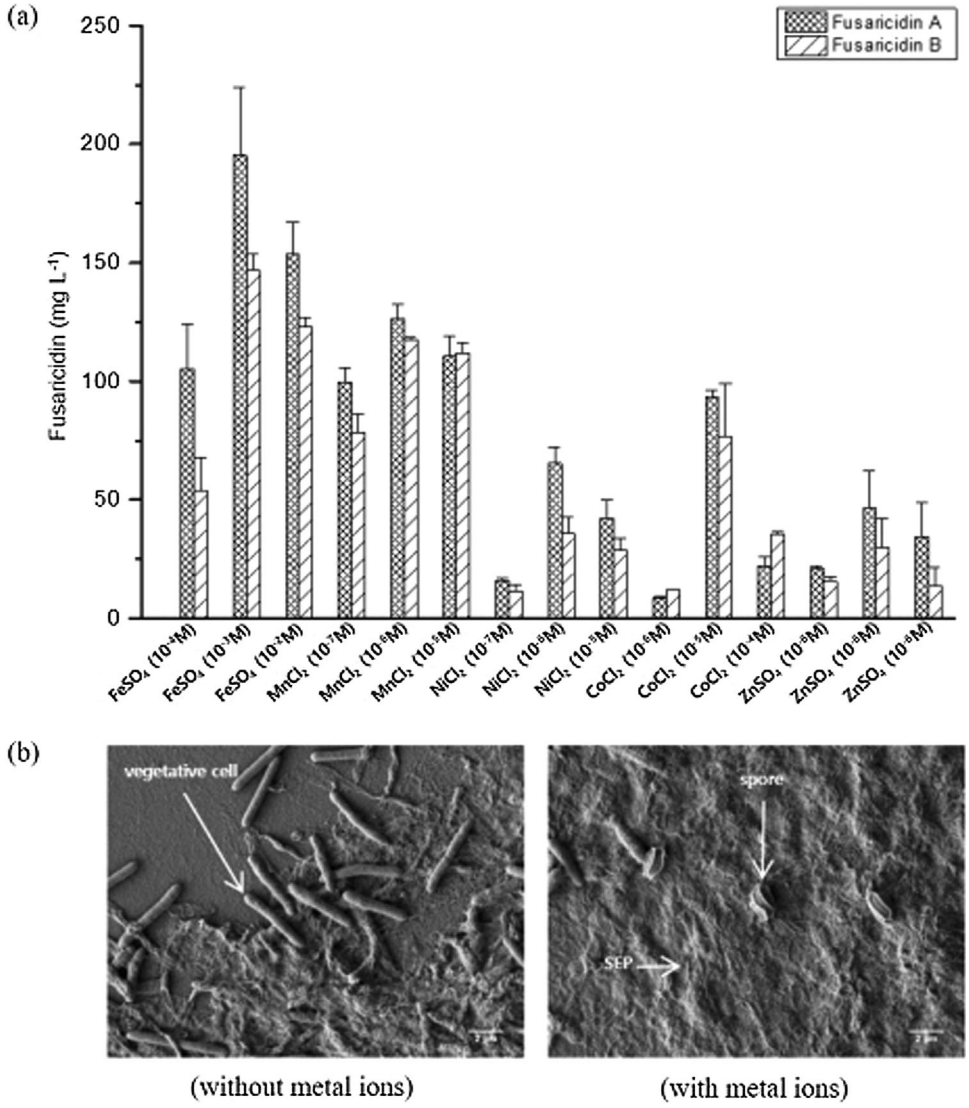

FIGURE 7 Effect of metal ions on the production of fusaricidins (a) and on the morphological changes of *P. kribbensis* CU01 (b). Bar size indicated 2 μm

Figure 7b, the addition of metal ions to the medium caused sporulation of *P. kribbensis* CU01 bacteria (Fig. 7b).

The effects of glucose concentration on fusaricidin production within the flask culture environment were also investigated. As glucose concentration in the M9 medium (containing 1×10^{-3} mol L^{-1} Fe^{2+} and 1×10^{-6} mol L^{-1} Mn^{2+}) increased to 20 g L^{-1}, the amount of fusaricidin A produced increased, whereas that of fusaricidin B was not significantly changed (Fig. 8). Interestingly, if metal ions such as Mn^{2+} and Fe^{2+} were not added to the medium, 20 g L^{-1} glucose did not significantly stimulate fusaricidin production. Maximum production concentrations of fusaricidin A and B were 460 and 118 mg L^{-1}, respectively, when 20 g L^{-1} of glucose was added to the M9 medium containing Mn^{2+} and Fe^{2+}. However, the maximum yield of fusaricidin A alone was obtained with the addition of 6 g L^{-1} glucose, and that of fusaricidin B was obtained with the addition of 4 g L^{-1} glucose.

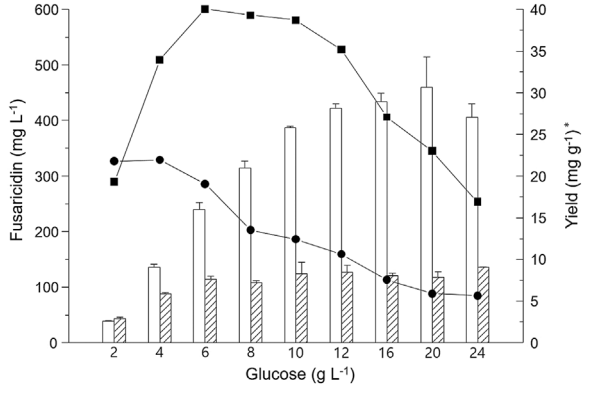

FIGURE 8 Effect of glucose on the production of fusaricidin A (□) and B (▨). Production yields of fusaricidin A (-■-) and B (-●-) were also shown. *The production of fusaricidin (mg) per glucose input (g)

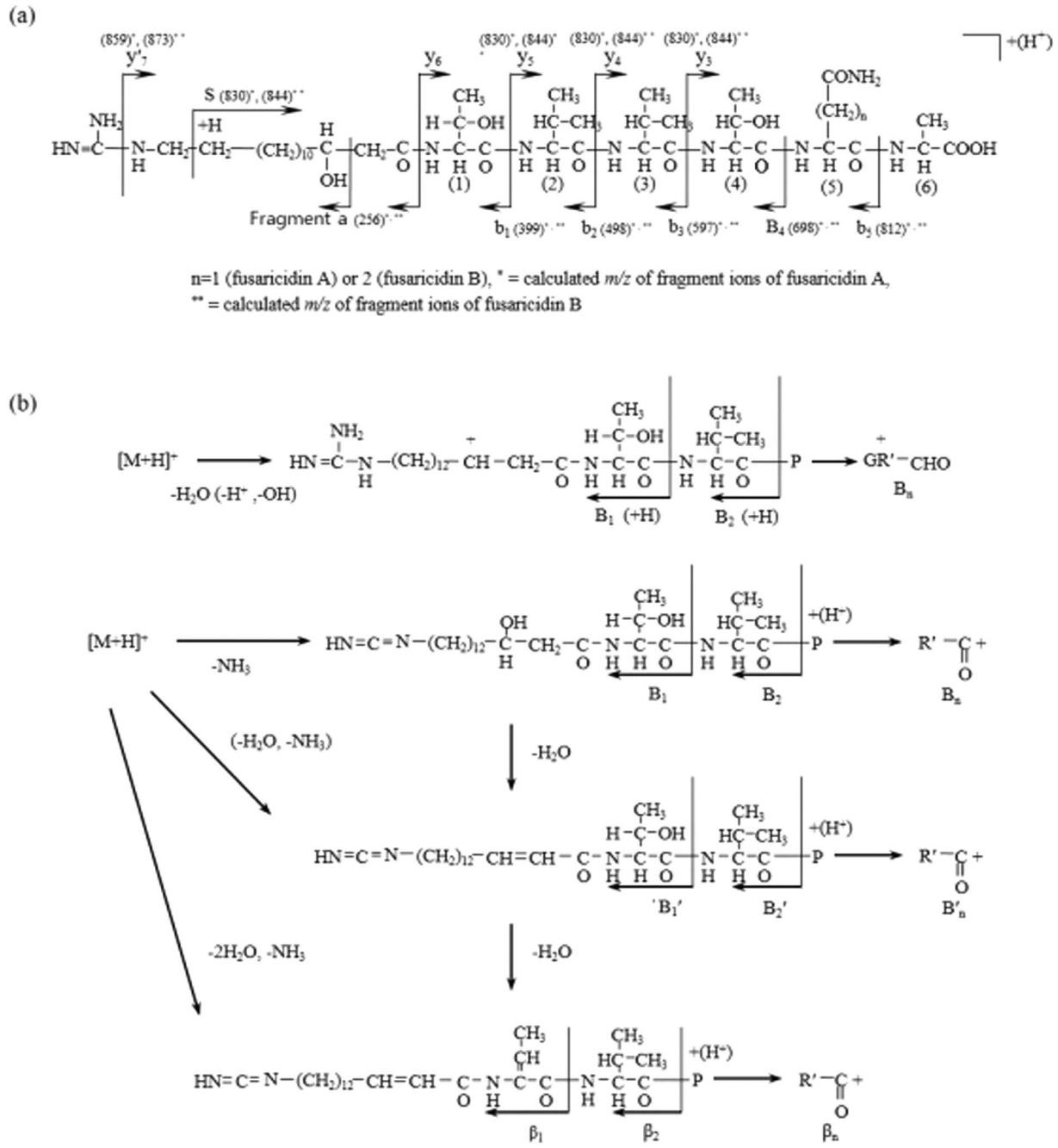

FIGURE 9 Fragments of b_n- and y_n- series (a) and fragments of B_n-, B'_n-, and β_n-series (b) produced from protonated molecules of linearized peptides, fusaricidin A and B[35]gr9

4 | DISCUSSION

The main chemical composition of yellow loess are as follows: 43-76% silica (SiO_2), 14-24% alumina (Al_2O_3), 1.4-12% ferric ion (Fe_2O_3), 0.28-1.1% titanium oxide (TiO_2), 0.01-0.12% manganese oxide (MnO), 0.03-2.6% calcium oxide (CaO), and 0.48-2.9% magnesium oxide (MgO) [4]. This indicates that yellow loess is a unique environmental habitat for growth of microorganisms. For this reason, we expected to reveal previously uncharacterized bacterial strains secreting novel antifungal substances in yellow loess.

Morphological and biochemical characteristics of the bacterial isolate selected by us for its potent antifungal activity were the same as those of *P. kribbensis* AM49^T (Table 1). Species within the current genus *Paenibacillus* had been originally assigned within the genus *Bacillus*, but were later reclassified as a separate genus [25]. The genus *Paenibacillus* consists of over 89 species of facultative anaerobes that belong to the category of endospore-forming, neutrophilic, and low G + C Gram-positive bacilli [26]. Many species of *Paenibacillus* have been demonstrated to have potential antifungal activities [3,27,28]. Strains of

Paenibacillus spp. were shown to produce diverse antimicrobial agents, including lantibiotics [29], lipopeptides [30], and macrolides [31]. *P. kribbensis* was reported as a new species of genus *Paenibacillus* [32], and some strains were found to produce antimicrobial substances. However, there have been no reports describing the structure of specific antimicrobial substances excreted from *P. kribbensis* [3,33].

In our experiments, antifungal substances were obtained from the extract of the mucoidal precipitate formed by *P. kribbensis* cultures, but not from the extract of the supernatant (Fig. 4). These results indicated that antifungal substances secreted by *P. kribbensis* CU01 at the stationary phase were not evenly diffused within the culture supernatant but rather were strongly bound to insoluble mucoidal polymers. Generally, antimicrobial substances produced by bacteria are soluble in the culture supernatant. However, in similarity to our observations, some antifungal substances produced by *P. polymyxa* JSa-9 were found to be tightly associated with either cells or cell wall-bound polymer [23]. Analysis of extracellular mucoidal polymers secreted by *P. kribbensis* CU01 using phenol-sulfuric acid method demonstrated that less than 50% (w/w) of the polymers consisted of polysaccharides. A more detailed analysis of the components of *P. kribbensis* mucoidal polymers will be the subject of our next study. As shown in Figure 4a, only two peaks were clearly observed in RP-HPLC chromatogram of the extract of mucoidal precipitate, and their corresponding fractions had strong antifungal properties. Other substances secreted by the cells into the culture medium were removed by low speed centrifugation. Therefore, it was easy to obtain highly pure samples of the antifungal substance by simple separation and *n*-butanol extraction. Only a small volume of *n*-butanol was needed to extract a small amount of mucoidal precipitate. From the perspective of the economic viability of commercial production, these are advantageous properties because they facilitate separation and purification of antifungal substances produced by *P. kribbensis* CU01.

Typically, CID-mode mass spectrometry generates y- and b-type fragment ions of linear peptides [34]. Thus, CID mass spectrometry is a useful tool for identifying amino acid sequence of linear peptides. It has been reported that protonated molecules linearized by alkaline hydrolysis produce many fragments following cleavage in CID conditions [35]. Generally, protonated forms are more amenable to fragmentation in CID- and LIFT-TOF/TOF experiments than the alkali adducts, showing a wealth of product ions that can be utilized for structural analysis [24]. For this reason, MS/MS analysis was performed on the linearized compound using LIFT-TOF/TOF. The MS/MS spectra results are consistent with the previously reported mass spectra of fusaricidin A and B [24,35] (Fig. 6). Figure 9a shows the production of b_n-(b_1-b_5) and y_n-series (y_3-y_6) ions from linearized fusaricidins. However, b_n- and y_n-series ions were observed only as weak peaks or were not detected in CID mass spectrometry measurements of their protonated molecules (Fig. 6). Figure 9b explains how linearized fusaricidin molecules produced B_n, B_n and β_n-series ions. Fortunately, most peaks of B_n- and B_n-series ions among the fragment ions appeared with a relatively strong intensity, so this spectrum made it easy to confirm the structure of fusaricidin (Fig. 6). Consequently, it was confirmed that *P. kribbensis* CU01 produces fusaricidin, which is a cyclic depsipeptide consisting of six amino acids and exhibiting a strong antimicrobial activity against fungi and Gram-positive bacteria [8,36].

As mentioned in the introduction, a variety of antifungal substances produced by bacteria are in many cases secondary metabolites, and their production yields can change depending on the types and concentrations of metal ions used. Raza et al. [18] have reported the importance of metal ions such as Ca^{2+}, Mn^{2+}, Ni^{2+}, and Cu^{2+} for the production of fusaricidins by *P. polymyxa*. Figure 7a shows that total fusaricidin production on flask culture scale was dramatically enhanced by the addition of Mn^{2+} and Fe^{2+} to M9 medium. Iron is known to be an essential metal ion for secondary metabolite production in bacteria. It is perhaps the most important micronutrient used by bacteria, which is required as a cofactor for a large number of enzymes and iron-containing proteins [37]. Mahmood [16] has already reported that Mn^{2+} and Fe^{2+}, both alone and together, enhance the growth and bulbiformin production of *B. subtilis*. Although in this study, high concentrations of iron significantly enhanced the production of fusaricidins, iron at such concentrations usually also inhibits cell growth. Presumably, high tolerance of *P. kribbensis* CU01 to iron may be related to the characteristics of its natural habitat, yellow loess, in which iron is present at high concentrations. In addition, metal ions stimulated cell sporulation (Fig. 7b). Beatty and Jensen [10] have reported that fusaricidins are produced at the beginning of sporulation by *P. polymyxa* PKB1. Ultimately, it was concluded that the production of fusaricidins was triggered by sporulation and significantly enhanced by metal ions.

In summary, we have isolated a bacterial strain with a strong antifungal activity, developed an inexpensive medium of its cultivation, and created a simple purification step facilitating potential commercialization of the mass production of fusaricidin. Investigations of the approaches to increase the maximum productivity, yield, as well as economical estimations at pilot-scale will be carried out in our next study.

ACKNOWLEDGMENTS

This study was supported by Bio-industry Technology Development Program 2012, Ministry for Food, Agriculture, Forestry, and Fisheries, Republic of Korea (Grant no. 112003-3). The study also received partial support from the Research Fund of the Chosun University (2014), Republic of Korea.

CONFLICTS OF INTEREST

All authors declare no financial or commercial conflicts of interest.

REFERENCES

[1] Bailey KL, Lazarovits G. Suppressing soil-borne diseases with residue management and organic amendments. Soil Tillage Res 2003;72: 169–80.

[2] Raposo R, Gomez V, Urrutia T, Melgarejo P. Fitness of *Botrytis cinerea* associated with dicarboximide resistance. Phytopathology 2000;90:1246–9.

[3] Xu SJ, Hong SJ, Choi W, Kim BS. Antifungal activity of *Paenibacillus kribbensis* strain T-9 Isolated from soils against several plant pathogenic fungi. Plant Pathol J 2014;30:102–8.

[4] Hwang JY, Jang MI, Kim JS, Cho WM. Mineralogy and chemical composition of the residual soils (Hwangto) from South Korea. J Miner Soc Korea 2000;13:147–63.

[5] Zeng Q, Dong Y, An S. Bacterial community responses to soils along a latitudinal and vegetation gradient on the loess plateau, China. PLoS ONE 2016;11:e0152894.

[6] Cochrane SA, Vederas JC. Lipopeptides from *Bacillus and Paenibacillus* spp.: a gold mine of antibiotic candidates. Med Res Rev 2016;36:4–31.

[7] Raza W, Yang X, Wu H, Wang Y. Isolation and characterisation of fusaricidin-type compound-producing strain of *Paenibacillus polymyxa* SQR-21 active against *Fusarium oxysporum* f.sp. nevium. Eur J Plant Pathol 2009;125:471–83.

[8] Kurusu K, Ohba K, Arai T, Fukushima K. New peptide antibiotics LI-F03, F04, F05, F07, and F08, produced by *Bacillus polymyxa*. I. isolation and characterization. J Antibiot (Tokyo) 1987;40:1506–14.

[9] Bionda N, Stawikowski M, Stawikowska R, Cudic M. Effects of cyclic lipodepsipeptide structural modulation on stability, antibacterial activity, and human cell toxicity. Chem Med Chem 2012;7:871–82.

[10] Beatty PH, Jensen SE. *Paenibacillus polymyxa* produces fusaricidin-type antifungal antibiotics active against *Leptosphaeria maculans*, the causative agent of blackleg disease of canola. Can J Microbiol 2002;48:159–69.

[11] Behal V. Proceedings of the 16th workshop conference hoescht, gracht castle. In: Kleinkauf H, von Dohren H, Dornaner H, Nesemann G, editors. Enzymes of secondary metabolism: regulation of their expression and activity. Weinheim, Germany: VCH Verlagsgerelle-shaft mbH; 1986. p. 265–81.

[12] Froyshov O, Mathiesen A, Haavik HI. Regulation of bacitracin synthetase by divalent metal ions in *Bacillus licheniformis*. J Gen Microbiol 1980;117:163–7.

[13] Paul AK, Banerjee AK. Determination of optimum conditions for antibiotic production by *Streptomyces galbus*. Folia Microbiol (Praha) 1983;28:397–405.

[14] Raytapadar S, Datta R, Paul AK. Effects of some heavy metals on growth, pigment and antibiotic production by *Streptomyces galbus*. Acta Microbiol Immunol Hung 1995;42:171–7.

[15] Weinberg ED. Biosynthesis of secondary metabolites: roles of trace metals. Adv Microb Physiol 1969;4:1–44.

[16] Mahmood M. Trace elements for growth and bulbiformin production by *Bacillus subtilis*. J Appl Bacteriol 1972;35:1–5.

[17] Morgenstern A, Paetz C, Behrend A, Spiteller D. Divalent transition-metal-ion stress induces prodigiosin biosynthesis in *Streptomyces coelicolor* M145: formation of coeligiosins. Chemistry 2015;21: 6027–32.

[18] Raza W, Hongsheng W, Qirong S. Use of response surface methodology to evaluate the effect of metal ions (Ca^{2+}, Ni^{2+}, Mn^{2+}, Cu^{2+}) on production of antifungal compounds by *Paenibacillus polymyxa*. Bioresour Technol 2010;101:1904–12.

[19] Raza W, Yang X, Wu H, Huang Q. Evaluation of metal ions (Zn^{2+}, Fe^{3+} and Mg^{2+}) effect on the production of fusaricidin-type antifungal compounds by *Paenibacillus polymyxa* SQR-21. Bioresour Technol 2010;101:9264–71.

[20] Deng Y, Lu Z, Lu F, Zhang C. Identification of LI-F type antibiotics and di-n-butyl phthalate produced by *Paenibacillus polymyxa*. J Microbiol Methods 2011;85:175–82.

[21] Nair D, Vanuopadath M, Nair BG, Pai JG. Identification and characterization of a library of surfactins and fengycins from a marine endophytic *Bacillus* sp. J Basic Microbiol 2016;56:1159–72.

[22] Yakimov MM, Timmis KN, Wray V, Fredrickson HL. Characterization of a new lipopeptide surfactant produced by thermotolerant and halotolerant subsurface *Bacillus licheniformis* BAS50. Appl Environ Microbiol 1995;61:1706–13.

[23] Deng Y, Lu Z, Bi H, Lu F. Isolation and characterization of peptide antibiotics LI-F04 and polymyxin B6 produced by *Paenibacillus polymyxa* strain JSa-9. Peptides 2011;32:1917–23.

[24] Vater J, Niu B, Dietel K, Borriss R. Characterization of novel fusaricidins produced by *Paenibacillus polymyxa*-M1 using MALDI-TOF mass spectrometry. J Am Soc Mass Spectrom 2015;26:1548–58.

[25] Ash C, Priest FG, Collins MD. Molecular identification of rRNA group 3 bacilli (Ash, Farrow, Wallbanks and Collins) using a PCR probe test. Proposal for the creation of a new genus *Paenibacillus*. Antonie van Leeuwenhoek 1993;64:253–60.

[26] Raza W, Yang W. Shen Q-R. *Paenibacillus polymyxa*: antibiotics, hydrolytic enzymes and hazard assessment. J Plant Pathol 2008;90: 419–30.

[27] Aktuganov G, Jokela J, Kivela H, Khalikova E. Isolation and identification of cyclic lipopeptides from *Paenibacillus ehimensis*, strain IB-X-b. J Chromatogr B Analyt Technol Biomed Life Sci 2014;973C:9–16.

[28] Naing KW, Lee YS, Nguyen XH, Jeong MH. Isolation and characterization of an antimicrobial lipopeptide produced by *Paenibacillus ehimensis* MA2012. J Basic Microbiol 2015;55:857–68.

[29] He Z, Kisla D, Zhang L, Yuan C. Isolation and identification of a *Paenibacillus polymyxa* strain that coproduces a novel lantibiotic and polymyxin. Appl Environ Microbiol 2007;73:168–78.

[30] Martin NI, Hu H, Moake MM, Churey JJ. Isolation, structural characterization, and properties of mattacin (polymyxin M), a cyclic

peptide antibiotic produced by *Paenibacillus kobensis* M. J Biol Chem 2003;278:13124–32.

[31] Wu XC, Qian CD, Fang HH, Wen YP. Paenimacrolidin, a novel macrolide antibiotic from *Paenibacillus* sp. F6-B70 active against methicillin-resistant *Staphylococcus aureus*. Microb Biotechnol 2011;4:491–502.

[32] Yoon JH, Oh HM, Yoon BD, Kang KH. *Paenibacillus kribbensis* sp. nov. and *Paenibacillus terrae* sp. nov., bioflocculants for efficient harvesting of algal cells. Int J Syst Evol Microbiol 2003;53:295–301.

[33] Cotta SR, da Mota FF, Tupinamba G, Ishida K. Antimicrobial activity of *Paenibacillus kribbensis* POC 115 against the dermatophyte *Trichophyton rubrum*. World J Microbiol Biotechnol 2012;28:953–62.

[34] Steen H, Mann M. The ABC's (and XYZ's) of peptide sequencing. Nat Rev Mol Cell Biol 2004;5:699–711.

[35] Kuroda J, Fukai T, Nomura T. Collision-induced dissociation of ring-opened cyclic depsipeptides with a guanidino group by electrospray ionization/ion trap mass spectrometry. J Mass Spectrom 2001;36: 30–7.

[36] Kajimura Y, Kaneda M, Fusaricidin A. A new depsipeptide antibiotic produced by *Bacillus polymyxa* KT-8. Taxonomy, fermentation, isolation, structure elucidation and biological activity. J Antibiotics. 1996;49:129–35.

[37] Leong SA, Expert D. Interactions—A molecular genetic perspective. In: Kosuge T, Nester E, editors. Siderophores in plant-pathogen interactions. New York: Academic Press; 1990. p. 62–83.

How to cite this article: Ryu J, Kim JM, Lee CW, Kim SW. Structural analysis and enhanced production of fusaricidin from *Paenibacillus kribbensis* CU01 isolated from yellow loess. *J Basic Microbiol*. 2017;57:525–535. https://doi.org/10.1002/jobm.201600692